2016 IEEE Innovative Smart Grid Technologies - Asia (ISGT-Asia)
Melbourne, Australia, Nov 28 - Dec 1, 2016

An AC-QP Optimal Power Flow Algorithm Considering Wind Forecast Uncertainty

Jennifer F. Marley, Maria Vrakopoulou, and Ian A. Hiskens

***Abstract*—While renewable generation sources provide many economic and environmental benefits for the operation of power systems, their inherent stochastic nature introduces challenges from the perspective of reliability. Existing optimal power flow (OPF) methods must therefore be extended to consider forecast errors to mitigate in an economic manner the uncertainty that renewable generation introduces. This paper presents an AC-QP OPF solution algorithm that has been modified to include wind generation uncertainty. We solve the resulting stochastic optimization problem using a scenario based algorithm that is based on randomized methods that provide probabilistic guarantees of the solution. The proposed method produces an AC-feasible solution while satisfying reasonable reliability criteria. Test cases are included for the IEEE 14-bus network that has been augmented with 2 wind generators. The scalability, optimality and reliability achieved by the proposed method are then assessed.**

***Index Terms*—AC optimal power flow, renewable generation, forecast uncertainty.**

I. Introduction

The increasing penetration of Renewable Energy Sources (RES) introduces challenges that require modifications to classical operational algorithms. A significant part of RES (e.g. wind and solar power) is associated with inherently intermittent generation, which is a major source of uncertainty in power systems. Uncertainty can create serious vulnerabilities in the reliable operation of power systems if not taken into account properly in the planning process. In this paper, we deal with the stochastic AC Optimal Power Flow (OPF) problem, and aim to find a solution that satisfies the non-convex constraints of the OPF problem while providing certain confidence on the constraint violation level due to the uncertain realizations of renewable generation.

The non-convex nature of the AC OPF problem has initiated the development of different algorithms that attempt to find an optimal solution in a scalable manner. The most commonly used simplification of the problem is the DC power flow approximation, which results in a quadratic program (QP) [1],[2]. This method achieves the scalability objective, as reliable solvers are readily available for large-scale QPs. However, the solution may not meet the desired reliability levels, due to the fact that it does not satisfy the AC power flow constraints [3]. Another more recent direction focuses on convex relaxations of the OPF problem, which result in semidefinite and second-order cone programs (SOCP) [4], [5]. These relaxations guarantee a globally optimal solution when tight; however, for arbitrary networks, tightness cannot be guaranteed [6],[7]. Moreover, current solvers do not support those problems in a scalable way. Another solution method is the AC-QP OPF algorithm [8], which is a successive linearization algorithm that alternates between solving a simple QP to minimize cost of generation and running an AC power flow to ensure AC-feasibility. This method has the benefit that it provides an AC-feasible solution, and moreover comes along with promising scalability properties, as the QP of the algorithm can be solved easily by current solvers even for very large networks. These benefits do, however, come with the tradeoff that the algorithm may converge to locally, rather than globally, optimal solutions and convergence cannot be guaranteed. Due to the fact that it guarantees an AC-feasible solution and scales better than the relaxation methods, this solution method forms the basis for this paper.

To address the uncertainty problem, we need to reformulate the AC OPF problem to provide a solution that satisfies the constraints in a probabilistic sense. There are many approaches that try to incorporate the stochasticity of the problem assuming the DC power flow model [9], [10], [11], [12], [13]. However, as mentioned above, the lack of AC feasibility may result in violation of the desired reliability levels. Numerous works consider the uncertainty by including in the optimization problem a certain set of scenarios that is heuristically chosen [9], [10], [11], usually using a scenario reduction technique. However, the latter does not provide any solution performance guarantees. Moreover, different directions look into analytical reformulations that mainly assume a closed form for the uncertainty distribution (e.g Gaussian) [13], [14] and hence can provide solutions with probabilistic performance. However, the uncertainty realizations (e.g wind power forecast errors) cannot be accurately described by analytical distributions, and moreover the complexity of those methods may increase dramatically when the non-convex OPF nature is considered. Furthermore, many formulations are based on robust optimization [15], where it is difficult to quantify the solution performance since (similar to the heuristic scenario techniques) the selected uncertainty set might end up being overly conservative or too risky.

This work was supported by the National Science Foundation through grants CNS-1238962 and CCF-1442495, and by the European Research Council under the European Unions Seventh Framework Programme (PIOF-GA-2013-626014).

J. Marley and I. Hiskens are with the Department of Electrical Engineering and Computer Science, University of Michigan, Ann Arbor, MI 48109, USA, jkfelder@umich.edu, hiskens@umich.edu.

M. Vrakopoulou is with the Department of Electrical Engineering and Computer Sciences, University of California, Berkeley, CA 94794, USA, mariavr@berkeley.edu.

978-1-5090-4302-6/16/$31.00 ©2016 IEEE

We seek an OPF methodology which finds solutions that come with guarantees, does not require a specific distribution of the uncertainty, and maintains reasonable complexity and solution time for real-time operation. Randomized optimization techniques like [16], [17], [18] satisfy those objectives. Those techniques are basically scenario based methods; however, their solution is a-priori guaranteed to satisfy the system constraints with certain probability. These techniques were first applied in the stochastic DC OPF problem in [12] and later, using the SDP relaxation of the power flow constraints, in the stochastic AC OPF in [19]. In this paper we will use the AC-QP OPF to achieve better scalability properties. As this is a non-convex problem, the methods in [16], [17] cannot be used, since they require the convexity of the underlying problem. Additionally, [18] cannot be practically applied since it requires finding the optimal solution of a robust counterpart of the initial problem, which cannot be easily achieved in the AC-QP OPF algorithm. We therefore rely on a recent algorithm presented in [20] that does not require convexity of the problem, but requires identifying the so called support set of the scenarios used in the optimization.

The remainder of the paper is organized as follows. Section II provides the formulation of the deterministic AC-QP OPF algorithm, introduces an extension of it to a scenario based formulation considering a finite number of scenarios of the uncertain variables, and proposes a probabilistic formulation of the problem that can provide a solution with a-posteriori performance guarantees. Section III then provides simulation results that validate the theoretical expectations, and conclusions are offered in Section IV.

II. AC-QP Probabilistic OPF Algorithm

A. Notation

The notation used in the formulation of a probabilistic optimal power flow (pOPF) is summarized in Table I.

TABLE I
NOTATION.

Control Variables:	
$\Delta P_{g,i}$	change in active power generation at node $i \in \mathcal{G}$
$\Delta Q_{g,i}$	change in reactive power generation at node $i \in \mathcal{G}$
ΔV_i, $\Delta\theta_i$	change in voltage magnitude, angle at node $i \in \mathcal{N}$
$\Delta Q^m_{g,i}$	change in reactive power generation at node $i \in \mathcal{G}$ in scenario $m \in \mathcal{S}$
ΔV^m_i, $\Delta\theta^m_i$	change in voltage magnitude, angle at node $i \in \mathcal{N}$ in scenario $m \in \mathcal{S}$
Parameters :	
$\mathcal{G}$	set of conventional generation nodes
$C_i(P_{g,i})$	quadratic cost curve for each generator $i \in \mathcal{G}$
$\mathcal{W}$	set of wind nodes
$\mathcal{S}$	set of wind power scenarios
$\mathcal{N}$	set of nodes in the network
d	participation vector of generators
$slack$	slack node in the network
pv	set of PV (generator) nodes in the network
$P_{w,i}$	base case wind forecast at node $i \in \mathcal{W}$
$P^m_{w,i}$	wind forecast at node $i \in \mathcal{W}$ in scenario $m \in \mathcal{S}$
S^{max}_{ij}	maximum apparent power flow in line from node i to node j
$P^{min}_{g,i}, P^{max}_{g,i}$	minimum, maximum active power limits when generator at node $i \in \mathcal{G}$ in service
$Q^{min}_{g,i}, Q^{max}_{g,i}$	minimum, maximum reactive power limits when generator at node $i \in \mathcal{G}$ in service
$\frac{\partial S_{ij}}{\partial\theta_k}, \frac{\partial S_{ij}}{\partial V_k}$	AC line flow sensitivity factors
J	AC power flow Jacobian matrix
V^{min}_i, V^{max}_i	minimum, maximum voltage magnitude at node $i \in \mathcal{N}$

B. Overview of the basic AC-QP OPF method

The AC-quadratic program OPF (AC-QP OPF) algorithm, which has been adopted from [8], is an iterative algorithm that consists of two parts. Firstly, an AC power flow is solved using an approximate initial operating point given by the solution of an SOCP relaxation of the AC OPF problem [4]. Secondly, a QP is solved to minimize the generation cost, while enforcing the linearized power balance and line flow constraints. The QP solution provides new generation and voltage schedules that are used in the next AC power flow. The AC power flow – QP iterations continue until the difference between the QP and power flow solutions agrees to within a specified tolerance (10^{-3} p.u. is considered sufficiently accurate in this case). A slight difference compared to [8] is that line flow constraints are only included in the QP for a subset of lines, rather than for all branches in the network. In practice, this has offered significant execution time and convergence improvements, as discussed in [21]. The modified algorithm is summarized in Fig. 1.

The QP solved at each iteration uses a linearization of the power balance and line flow constraints around the previous AC power flow solution. To do so, the Jacobian of the power flow equations, $\mathbf{J}$, as well as the line-flow sensitivity factors $\frac{\partial S_{ij}}{\partial\theta_k}$ and $\frac{\partial S_{ij}}{\partial V_k}$ are updated after each power flow. To improve convergence, a "trust-region" step based on the formulation in [22] is added to check the accuracy of this linearization before the QP is solved; the details of this step can be found in [21].

The superscript '$\circ$' denotes values obtained from the converged AC power flow, which are updated after each AC power flow computation. The notation Δ denotes a change from the converged power flow value of the corresponding variable at the current iteration of the AC-QP algorithm.

The QP is then formulated as:

$$\min \sum_{i\in\mathcal{G}} C_i\big(P^\circ_{g,i} + \Delta P_{g,i}\big) \quad \text{subject to} \tag{1a}$$

$$\mathbf{J}\Delta x = \Delta S \tag{1b}$$

$$P^{min}_{g,i} \le P^\circ_{g,i} + \Delta P_{g,i} \le P^{max}_{g,i} \qquad \forall i \in \mathcal{G} \tag{1c}$$

$$Q^{min}_{g,i} \le Q^\circ_{g,i} + \Delta Q_{g,i} \le Q^{max}_{g,i} \qquad \forall i \in \mathcal{G} \tag{1d}$$

$$\Delta\theta_{slack} = 0 \tag{1e}$$

$$V^{min}_i \le V^\circ_i + \Delta V_i \le V^{max}_i \qquad \forall i \in \mathcal{N} \tag{1f}$$

$$S^\circ_{ij} + \sum_{k\in\mathcal{N}} \frac{\partial S_{ij}}{\partial\theta_k}\Delta\theta_k + \sum_{k\in\mathcal{N}} \frac{\partial S_{ij}}{\partial V_k}\Delta V_k \le S^{max}_{ij} \qquad \forall\,(i,j) \in \mathcal{L}^* \text{ and } \forall\,(j,i) \in \mathcal{L}^* \tag{1g}$$

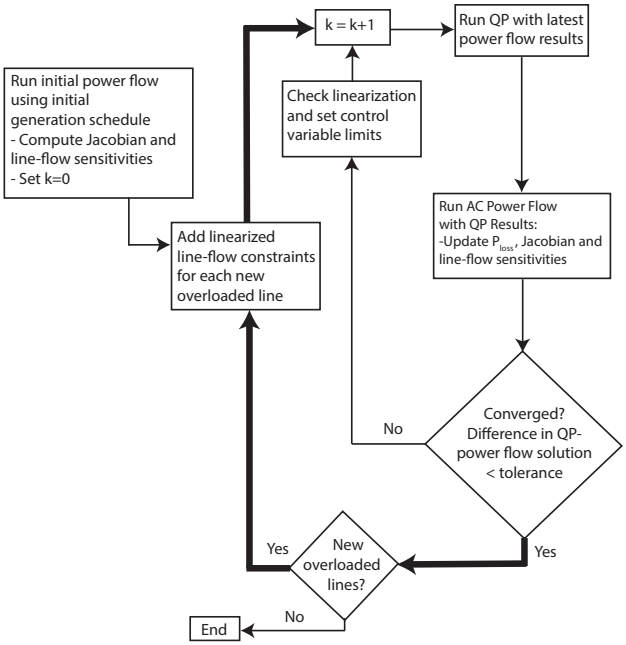

Fig. 1. AC-QP OPF algorithm.

where

$$\mathbf{J} = \begin{bmatrix} \frac{\partial P}{\partial \theta} & \frac{\partial P}{\partial V} \\ \frac{\partial Q}{\partial \theta} & \frac{\partial Q}{\partial V} \end{bmatrix}, \qquad \Delta x = \begin{bmatrix} \Delta\theta \\ \Delta V \end{bmatrix}, \qquad \Delta S = \begin{bmatrix} \Delta P_g \\ \mathbf{0} \\ \Delta Q_g \\ \mathbf{0} \end{bmatrix}$$

where the $\mathbf{0}$ entries in ΔS correspond to non-generator buses.

The cost function $C_i(\cdot)$ is a quadratic function of the conventional generation dispatch, $P^{\circ}_{g,i} + \Delta P_{g,i}$, and is minimized subject to the linearized power balance constraints (1b), generation active and reactive power limits (1c),(1d), bus voltage magnitude limits (1f), and linearized line flow limits (1g). Constraint (1e) represents the reference angle, restricting our solution to a finite solution space. Note that the linearized line-flow constraints (1g) are initially enforced for all lines that are at or above 95% of their line-flow limit, the set of which is denoted $\mathcal{L}^*$. This set is then updated at the beginning of each outer loop of the AC-QP algorithm to include any lines that are overloaded but have not yet been added to the set (bolded in Fig. 1).

C. Introducing scenarios into the AC-QP OPF

The solution of the AC-QP OPF of the previous subsection is deterministic in the sense that it does not take into account the uncertainties of the system. In this subsection, we consider wind power uncertainty, and we reformulate the algorithm shown in Fig. 1 to provide a solution that is robust over a finite set of possible wind power scenarios. This results in a probabilistic AC-QP OPF algorithm (AC-QP pOPF). The base case generation dispatch will satisfy the balance constraints for a given wind power forecast. Any wind power scenario differing from the forecast will then drive the system to a new operating point due to the created generation-load mismatch. This power mismatch is assumed to be compensated by adjusting the power of the generators based on a distribution (or participation) percentage vector [12], [8]. Each scenario will also incur different losses in the network, so the generated power should be adjusted accordingly to cover this loss variation. Note that here we have assumed the generator voltages remain constant through deviations from the wind power forecast.

The robust (over the scenarios) reformulation is again based on a series of iterations between an AC power flow and a QP, as in the deterministic algorithm shown in Fig. 1. The initialization of the AC power flow is now given by a reformulation of the SOCP relaxation where constraints are added for each new operating point due to a scenario. This reformulation takes into account, through the distribution vector, the coupling of the generation dispatch between the base case (wind power forecast) and all the scenario cases. This ensures an appropriate distribution of the wind power forecast error to the generators. After the QP is solved, a separate AC power flow is solved for the base case and each scenario. In all cases, the power dispatch is adjusted according to the distribution factors to meet the network losses. Within the QP, a separate linearization is formed for each scenario, with the Jacobian matrix and line flow sensitivities obtained from the corresponding power flow.

Let $\mathcal{S}$ represent the set of scenarios to be included in the optimization problem. For every scenario $m \in \mathcal{S}$, we add the following set of operational constraints in line with the base case description (1b)-(1g):

$$\tilde{\mathbf{J}}^{\mathbf{m}} \Delta x^m = \Delta S^m \tag{2a}$$

$$P^{min}_{g,i} \le P^{\circ,m}_{g,i} + \Delta P_{g,i} \le P^{max}_{g,i} \qquad \forall i \in \mathcal{G} \tag{2b}$$

$$Q^{min}_{g,i} \le Q^{\circ,m}_{g,i} + \Delta Q^{m}_{g,i} \le Q^{max}_{g,i} \qquad \forall i \in \mathcal{G} \tag{2c}$$

$$\Delta\theta^m_{slack} = 0 \tag{2d}$$

$$V_i^{min} \le V_i^{\circ,m} + \Delta V_i^m \le V_i^{max} \qquad \forall i \in \mathcal{N} \tag{2e}$$

$$\Delta V_i = \Delta V_i^m \qquad \forall i \in \mathcal{G} \tag{2f}$$

$$S^{\circ,m}_{ij} + \sum_{k\in\mathcal{N}} \frac{\partial S_{ij}}{\partial \theta_k}^m \Delta\theta^m_k + \sum_{k\in\mathcal{N}} \frac{\partial S_{ij}}{\partial V_k}^m \Delta V^m_k \le S^{max}_{ij}$$
$$\forall\,(i,j) \in \mathcal{L}^{*,m} \text{ and } \forall\,(j,i) \in \mathcal{L}^{*,m}. \tag{2g}$$

The modified linearization for each scenario is given by

$$\tilde{\mathbf{J}}^{\mathbf{m}} = \begin{bmatrix} \frac{\partial P}{\partial \theta}^m & 0 \\ 0 & \frac{\partial Q}{\partial V}^m \end{bmatrix}, \Delta x^m = \begin{bmatrix} \Delta\theta^m \\ \Delta V^m \end{bmatrix}, \Delta S^m = \begin{bmatrix} \Delta P_g \\ \mathbf{0} \\ \Delta Q^m_g \\ \mathbf{0} \end{bmatrix}.$$

Each scenario m introduces extra variables, namely the reactive power output of each generator (ΔQ^m_g) and the voltage at each bus (ΔV^m, $\Delta\theta^m$). We force the deviation of the active power generation, ΔP_g, to take the same value for the base case and all scenarios. Note that the mismatch due to the scenarios is already incorporated in the generation dispatch, $P^{\circ,m}_g$, obtained from the previous AC power flow. Moreover, we enforce the same generator voltage magnitude setpoints in the base case and each scenario through constraint (2f).

Once the algorithm has converged, the final solution guarantees that the operating point of the base case and the operating

points for the considered scenarios will satisfy the non-convex AC power flow constraints. However, there is no guarantee that the constraints will be satisfied for arbitrary scenarios. To achieve generalization properties, we will employ a randomized optimization technique, which is presented in Section II-E.

D. Improving the scalability of the AC-QP pOPF

The previous subsection presented the pOPF for the general case where a finite number of wind power scenarios are considered. To make this method more scalable with respect to the number of scenarios that can be incorporated, the modified algorithm shown in Fig. 2 is proposed. This algorithm is based on ranking the scenarios according to the absolute value of the difference between the scenario and the forecast, $|\sum_{i\in\mathcal{W}}(P^m_{w,i} - P_{w,i})|$. This updated method adds only the highest ranked wind scenario to the pOPF at the beginning of each outer loop. Then, if the solution results in constraint violations for any of the remaining scenarios, one more scenario from those with violations is added in the same way to the pOPF at the next iteration. In practice, we have observed that relatively few of these outer loops are necessary to satisfy the constraints for even a very large number of scenarios. Limiting the size of the subset of wind power scenarios explicitly added to the pOPF problem reduces the number of variables and constraints in the QP, making the AC-QP pOPF faster to achieve a feasible solution for all the considered scenarios.

E. Providing a-posteriori probabilistic guarantees

The algorithm presented in the previous subsection can provide a feasible solution to the pOPF problem for a large number of scenarios. At the same time, we identify a very small number of scenarios with which the algorithm provides an identical feasible solution. This is a crucial property of the algorithm, since it implies that a feasible solution generated from a small fraction of the available scenarios exhibits good generalization properties. It results in zero empirical probability of constraint violation, i.e, it satisfies the constraints for all other scenarios even though they were not used when constructing the solution [23].

The recently presented work in [20] provides a framework for finding a solution of a non-convex problem that is accompanied with a-posteriori probabilistic guarantees. This method can be applied to any algorithm that takes as input a certain set of scenarios and provides a feasible solution of the problem. The critical point is the definition of the support set, also known as a compression scheme in [23], which is the set of scenarios that support the solution. In other words, if we consider the solution of the problem using a set of N scenarios $\mathcal{S}_N$, and we can achieve the same exact solution given a subset $\mathcal{S}_k$ of $\mathcal{S}_N$ that contains only k scenarios, the set $\mathcal{S}_k$ is a support set of the problem with N scenarios.

In [20], given that we can identify the cardinality k of the support set of the problem associated with N scenarios, a theoretical upper bound of the probability of constraint violation is provided by the formula:

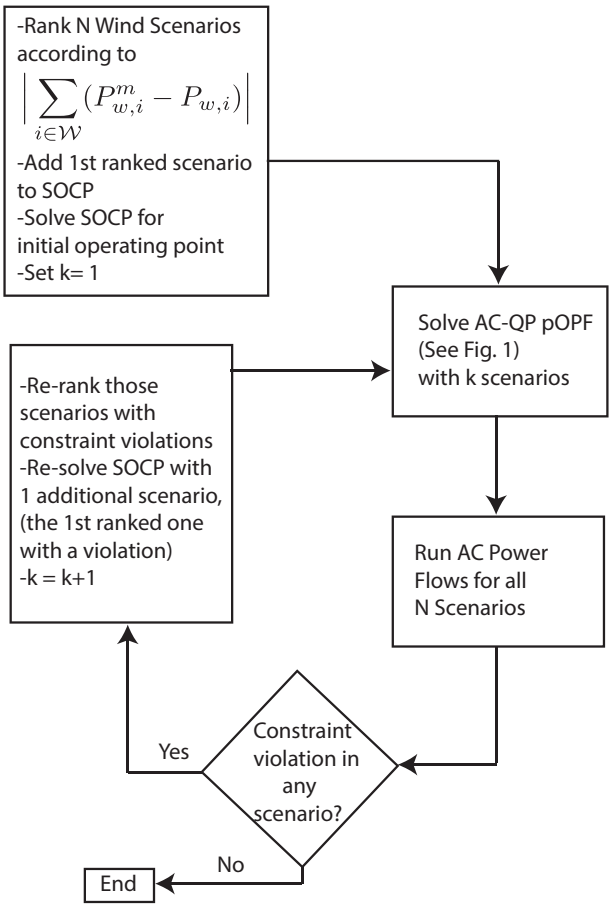

Fig. 2. AC-QP pOPF algorithm for N scenarios.

$$\epsilon(k) = \begin{cases} 1, & \text{if } k = N \\ 1 - \sqrt[N-k]{\frac{\beta}{N\binom{N}{k}}}, & \text{otherwise} \end{cases} \tag{3}$$

where $\beta \in (0, 1)$ is a design parameter that represents the probability that the upper bound ϵ will be violated. In other words, β is the probability that the probability of constraint violation will be greater that ϵ. By choosing a very small β (e.g. $\beta = 10^{-4}$), the bound ϵ is true with "very high confidence".

The only assumptions required for this to hold are that the algorithm should map the scenario set to a 'unique' solution that satisfies the constraints for all the scenarios in the set, and that the solution is invariant to any permutation of the scenarios taken into account. Both requirements are satisfied for the proposed algorithm.

Since we can only identify the cardinality of the support set after obtaining the solution, the provided guarantees are only a-posteriori. The result will be less conservative if the support set with minimum cardinality is identified.

In the following section, we will use the algorithm proposed in Section II-D to obtain a solution, identify the cardinality of the support set, and validate the aforementioned theoretical

probabilistic bound via Monte Carlo simulations.

III. Results and Discussion

A. An indicative example of the AC-QP pOPF

A first test case that uses the IEEE 14-bus network and unit commitment [24] is presented to demonstrate the progression of this method when including 1500 scenarios in the pOPF, and how the resulting support set for this problem is identified. The network has been augmented with two wind generators at nodes 9 and 3; 40 MW of available wind power is assumed at each node in the base case forecast. This corresponds to a renewable penetration (calculated as the ratio of total available wind generation to total generation capacity) of 9.4%. The AC-QP method described in Fig. 2 is used to consider 1500 scenarios. The results are shown in Fig. 3.

The method begins by randomly choosing 1500 scenarios from a set of 10,000 possible scenarios. These 1500 scenarios are then ranked according to the criterion established in Section II-D, the absolute value of the total mismatch. An SOCP relaxation is solved including only the first scenario, which corresponds to the scenario with the largest total mismatch, to initialize the AC-QP algorithm. That single scenario is also included in the QP of the AC-QP algorithm. After the AC-QP method has terminated, an AC power flow is run for all 1500 scenarios being considered, and the set of scenarios with constraint violations is identified.

After the AC-QP terminated with only one scenario included, running the AC power flow for all 1500 scenarios revealed that there are 226 scenarios with constraint violations. This is shown as the initial point in the upper plot of Fig. 3. These 226 scenarios are again sorted with respect to the absolute mismatch criterion, and the first ranked scenario (again corresponding to the scenario with the largest mismatch that has constraint violations) is now added to the set of scenarios included in the AC-QP. The SOCP relaxation is again solved, now with two scenarios, to reinitialize the AC-QP algorithm. The process repeats, adding a single scenario to the AC-QP in each outermost loop of the algorithm. This process identifies a very small number of scenarios that must be explicitly included in the AC-QP such that constraints are satisfied for all 1500 scenarios.

For this example, only 4 scenarios out of the 1500 possibilities needed to be included in the AC-QP such that the resulting solution satisfied the constraints for all 1500 scenarios. In other words, using just the 4 scenarios gave an identical feasible solution to the problem that incorporated all 1500 scenarios. This further implies that the 4 scenarios comprise the support set for this particular case. The resulting solution is accompanied with a-posteriori probabilistic guarantees. Since we have a feasible solution for the 1500 scenarios and we identified that the same feasible solution exists for only 4 of the scenarios, we can claim with very high confidence ($\beta = 10^{-4}$) that the solution of our algorithm will satisfy the system constraints with probability at least 97.2% over any possible realization of the wind power. In fact, Monte-Carlo simulation revealed that the empirical probability of violation in this case is only 0.23%. The empirical violation probability is evaluated by checking the violation of the constraints for 10000 scenarios. The scenarios are generated by a Markov Chain Monte Carlo (MCMC) mechanism which builds a transition probability matrix that suggests with what probability the uncertain variables will move from one value to another in time [25]. To train the model we used normalized hourly measured wind power data, both forecasts and actual values, for the total wind power infeed of Germany over the period 2006-2011.

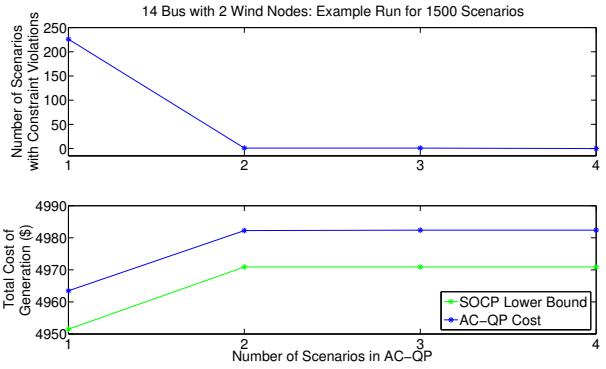

Fig. 3. Solving pOPF with 1500 scenarios.

The lower plot of Fig. 3 shows the AC-QP cost and corresponding SOCP lower bound after each additional scenario is added. These results demonstrate the tradeoff between reliability and optimality: each additional scenario increases the cost of operation, until constraints have been satisfied for all 1500 scenarios and no further scenarios need be included in the pOPF. Additionally, we notice that the AC-QP cost results are sufficiently close to the SOCP lower bound, and therefore also sufficiently close to the globally optimal solution.

B. Extended results

The previous example using the modified IEEE 14-bus network is now expanded to assess the performance of the proposed AC-QP pOPF method as the numbers of scenarios included in the pOPF problem (the value of N in Fig. 2) is increased from 10 to 1500[1]. The choice of 1500 scenarios here is sufficiently large to explore the impact on the empirical probability of violation of increasing numbers of scenarios included in the pOPF problem. The quality of solution from the AC-QP pOPF algorithm is assessed via Monte Carlo simulations using 10,000 possible scenarios. For each scenario, an AC power flow is run and the violation of any constraint is checked. Out of those 10,000 scenarios, those that result in any constraint violations (including generator active and reactive power limits, voltage magnitude limits, and line flow limits) are recorded to provide an empirical probability of constraint violation. For each choice of N, the number of scenarios included in pOPF,

[1]Recall that the N=1500 case was presented in Section III-A.

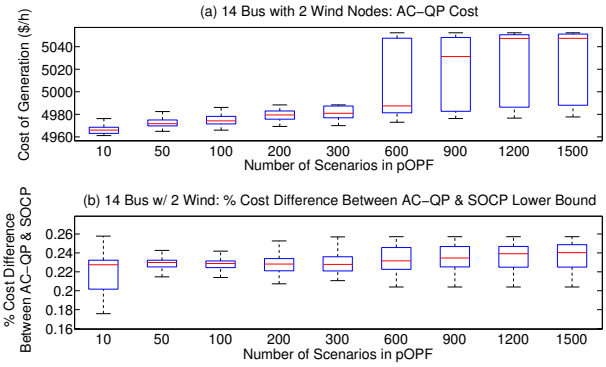

Fig. 4. (a) Cost of generation, (b) Distance from SOCP lower bound results.

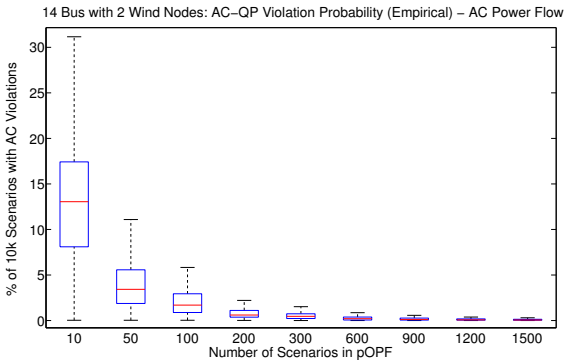

Fig. 5. AC-QP empirical violation.

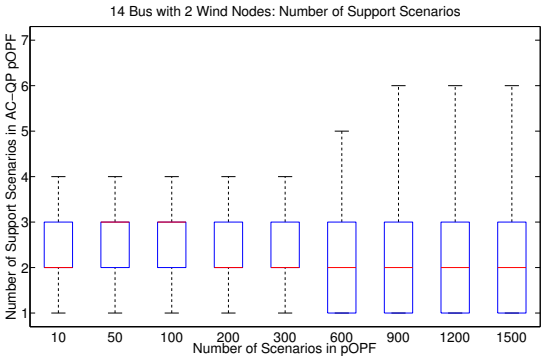

Fig. 6. Number of support scenarios.

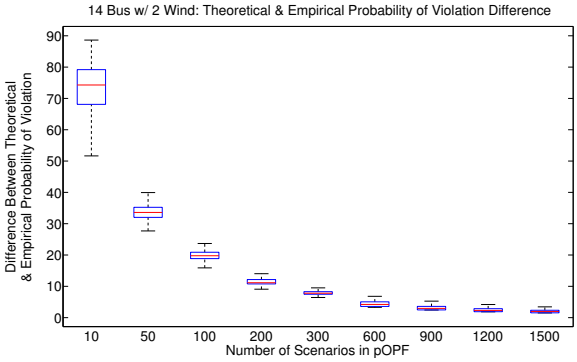

Fig. 7. Empirical violation compared to a-posteriori theoretical violation.

500 repeated trials are then performed[2], where each trial differs in the specific set of N randomly chosen wind power scenarios that are included in the pOPF problem.

The generation cost results and the corresponding empirical probability of constraint violation are shown in Fig. 4(a) and Fig. 5 respectively, for increasing N. These figures demonstrate the inherent tradeoff between reliability and optimal cost of operation. As more scenarios are included in the pOPF problem, the cost of operation increases, resulting in a less economic operating point. However, with an increasing number of scenarios added to the algorithm, the solution is more robust and fewer scenarios create constraint violations. Thus, although less economic, operating points that consider larger numbers of scenarios in the pOPF are more reliable. Furthermore, Fig. 4(b) validates the quality of solution of these results: the cost of generation in all cases is within 0.26% of the SOCP lower bound, and is thus sufficiently close to the globally optimal solution.

The empirical probability of violation in Fig. 5 does in fact decrease significantly as the number of scenarios included in the pOPF algorithm increases. Notice that with only 50 scenarios included in the pOPF problem, the empirical probability of violation is already below 5% for 75% of the trials.

Based on the theory discussed in Section II-E, the solution of the proposed algorithm should verify the a-posteriori probabilistic guarantees. To assess this, we identify the cardinality of the support set for each case study and then calculate the upper theoretical violation bound based on (3). Fig. 6 summarizes the cardinality of the support set for each case study. As these results show, a very small number of scenarios, on average around 2, need to be explicitly enforced in the AC-QP problem for all constraints to be satisfied for the remaining scenarios.

A comparison between the empirical and theoretical violation results is shown in Fig. 7, where the y-axis gives the theoretical minus the empirical probability of violation. We observe a positive difference, which highlights that the solution of the AC-QP pOPF algorithm results in an empirical probability of violation that is always satisfying the theoretical bounds.

To ensure the reliability of a system, large numbers of scenarios may need to be included in the pOPF problem. The scalability of any proposed algorithm is therefore an important factor that must be assessed. For the purposes of real-time operation, a threshold of 5 minutes (300 seconds) is assumed to be an acceptable limit on total execution time. Figure 8 summarizes the timing results for the proposed AC-QP pOPF

[2]The results are gathered in boxplots which give several statistical quantities of interest for each set of 500 trials, given the number of scenarios to be included in the pOPF: the central line inside the box shows the median over all 500 trials; the bottom and top edges of each box show the 25% and 75% percentiles respectively; and the vertical lines show the extreme values.

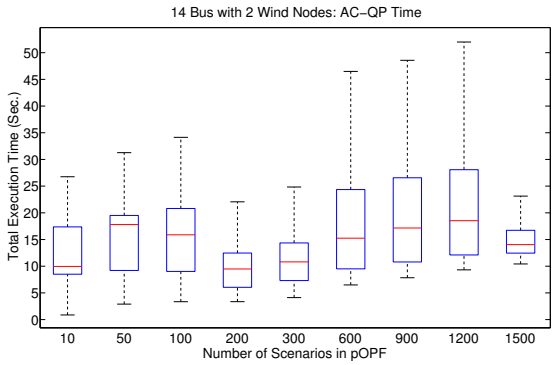

Fig. 8. AC-QP timing results.

algorithm. As these results show, the timing requirement is clearly satisfied even for the 1500 scenario case, which has an average solution time of less than 20 seconds. These results suggest the proposed method scales well with the number of scenarios included in the pOPF problem. In general, the algorithm is promising with respect to scalability properties over the network size since it involves simple, not substantially time-consuming steps. Future work will further investigate the practical limits of the algorithm.

IV. Conclusions

The AC-QP OPF solution method has been extended to include wind power uncertainty, captured through the addition of a finite number of possible wind scenarios. The scalability of this algorithm with respect to large numbers of scenarios has been demonstrated, and the timing results support its utility for real-time applications. A modified SOCP with wind scenarios is used both to initialize the AC-QP method and to assess the optimality of the resulting solution. The algorithm fits in the framework of a randomized optimization technique that can characterize the solution with a-posteriori theoretical probabilistic guarantees. The empirical reliability of the solution has been evaluated to assess the quality of the AC-QP solution and verify the theoretical bound.

The modified AC-QP pOPF algorithm offers several advantages. Firstly, it does not rely upon model approximations as in DC OPF formulations. Secondly, it produces an AC feasible solution, where convex relaxations may not be tight. Thirdly, it maintains scalability with respect to the number of scenarios to be optimized over, which is a limitation of convex relaxations. Finally, it provides a probabilistically robust solution with a-posteriori probabilistic violation guarantees.

References

[1] A. Motto, F. Galiana, A. Conejo, and J. Arroyo, "Network-Constrained Multiperiod Auction for a Pool-Based Electricity Market," *IEEE Transactions on Power Systems*, vol. 17, no. 3, pp. 646–653, Aug. 2002.

[2] T. Overbye, X. Cheng, and Y. Sun, "A Comparison of the AC and DC Power Flow Model for LMP Calculations," in *37th Hawaii Int. Conf. Syst. Sci. (HICSS)*, Jan. 2006.

[3] B. Stott, J. Jardim, and O. Alsac, "DC Power Flow Revisited," *IEEE Transactions on Power Systems*, vol. 24, no. 3, pp. 1290–1300, Aug. 2009.

[4] S. Low, "Convex Relaxation of Optimal Power Flow–Part I: Formulations and Equivalence," *IEEE Transactions on Control of Network Systems*, vol. 1, no. 1, pp. 15–27, March 2014.

[5] J. Lavaei and S. Low, "Zero Duality Gap in Optimal Power Flow Problem," *IEEE Transactions on Power Systems*, vol. 27, no. 1, pp. 92–107, Feb. 2012.

[6] B. Lesieutre, D. Molzahn, A. Borden, and C. DeMarco, "Examining the Limits of the Application of Semidefinite Programming to Power Flow Problems," in *49th Annu. Allerton Conf. Commun., Control, Comput.*, Sept. 2011, pp. 1492–1499.

[7] D. Molzahn, B. Lesieutre, and C. DeMarco, "Investigation of Non-Zero Duality Gap Solutions to a Semidefinite Relaxation of the Optimal Power Flow Problem," in *47th Hawaii Int. Conf. Syst. Sci. (HICSS)*, 6-9 Jan. 2014.

[8] A. Wood, B. Wollenberg, and G. Sheble, *Power Generation, Operation and Control*, 3rd ed. John Wiley and Sons, Inc., 2013.

[9] F. Bouffard and F. F. Galiana, "Stochastic security for operations planning with signiffcant wind power generation," *IEEE Transactions on Power Systems*, vol. 23, no. 2, pp. 306–316, 2008.

[10] A. Papavasiliou, S. Oren, and R. ONeill, "Reserve requirements for wind power integration: A scenario-based stochastic programming framework," *IEEE Transactions on Power Systems*, vol. 26, no. 4, pp. 2197–2206, 2011.

[11] J. Morales, A. Conejo, and J. Perez-Ruiz, "Economic valuation of reserves in power systems with high penetration of wind power," *IEEE Transactions on Power Systems*, vol. 24, no. 2, pp. 900–910, 2009.

[12] M. Vrakopoulou, K. Margellos, J. Lygeros, and G. Andersson, "Probabilistic guarantees for the N-1 security of systems with wind power generation," in *Probabilistic Methods Applied to Power Systems Conference*, 2012.

[13] L. Roald, F. Oldewurtel, T. Krause, and G. Andersson, "Analytical Reformulation of Security Constrained Optimal Power Flow with Probabilistic Constraints," in *IEEE PowerTech Conference*, 2013.

[14] D. Bienstock, M. Chertkov, and S. Harnett, "Chance-constrained optimal power flow: Risk-aware network control under uncertainty," *SIAM Review*, vol. 56, no. 3, pp. 461–495, 2014.

[15] D. Bertsimas, E. Litvinov, X. Sun, J. Zhao, and T. Zheng, "Adaptive robust optimization for the security constrained unit commitment problem," *IEEE Transactions on Power Systems*, vol. 28, no. 1, pp. 52–62, 2013.

[16] G. Calafore and M. C. Campi, "The scenario approach to robust control design," *IEEE Transactions on Automatic Control*, vol. 51, no. 5, pp. 742–753, 2006.

[17] T. Alamo, R. Tempo, and A. Luque, "On the sample complexity of randomized approaches to the analysis and design under uncertainty," *Proceedings of the American Control Conference*, 2010.

[18] K. Margellos, P. Goulart, and J. Lygeros, "On the road between robust optimization and the scenario approach for chance constrained optimization problems," *IEEE Transactions on Automatic Control*, vol. 59, no. 8, pp. 2258–2263, 2014.

[19] M. Vrakopoulou, M. Katsampani, K. Margellos, J. Lygeros, and G. Andersson, "Probabilistic security-constrained AC optimal power flow," in *IEEE PowerTech Conference*, 2013.

[20] M. Campi, S. Garatti, and F. Ramponi, "Non-convex scenario optimization with application to system identification," in *54th IEEE Conference on Decision and Control*, 2015.

[21] J. F. Marley, D. K. Molzahn, and I. A. Hiskens, "An improved initialization for the AC-QP OPF method using an SOCP relaxation," *IEEE Transactions on Power Systems*, submitted.

[22] A. M. Giacomoni and B. F. Wollenberg, "Linear Programming Optimal Power Flow Utilizing a Trust Region Method," in *North Amer. Power Symp.*, 2010.

[23] K. Margellos, M. Prandini, and J. Lygeros, "On the connection between compression learning and scenario based single-stage and cascading optimization problems," *IEEE Transactions on Automatic Control*, vol. 60, no. 10, pp. 2716–2721, 2015.

[24] R. Zimmerman, C. Murillo-Sánchez, and R. Thomas, "MATPOWER: Steady-State Operations, Planning, and Analysis Tools for Power Systems Research and Education," *IEEE Trans. Power Syst.*, no. 99, pp. 1–8, 2011.

[25] G. Papaefthymiou and B. Klöckl, "MCMC for wind power simulation," *IEEE Transactions on Energy Conversion*, vol. 23, no. 1, pp. 234–240, 2008.